Volume 6, Issue 3, July 2019 ISSN: 2348-8565 (Online)

International Journal of Modern Engineering and Research Technology

Website: http://www.ijmert.org Email: editor.ijmert@gmail.com

Spectroscopic (FT-IR, FT-Raman, FT-NMR and UV-VIS) Investigation on 4-Benzyloxy-3-Methoxybenzaldehyde using Quantum

A. Parathasarathi
Ph.D. Research Scholar (Physics)
A.V.C. College [Autonomous]),
Mayladuthurai, (Tamilnadu) [INDIA]
Email: sheelaraj051990@gmail.com

K. Jayasheela
Ph. D, Research Scholar (Physics)
Kanchi Mamunivar Center for Post graduate Studies [Autonomous])
Lawspet (Pondicherry) [INDIA]
Email: sheelaprabha24@gmail.com

T. Prabhu
Assistant Professor (Physics)
A.V.C. College [Autonomous]),
Mayladuthurai, (Tamilnadu) [INDIA]
Email: ttsprabhu@gmail.com

S. Periandy
Assistant Professor (Physics)
Kanchi Mamunivar Center for Post graduate Studies [Autonomous])
Lawspet (Pondicherry) [INDIA]
Email: sarathigangai@gmail.com

ABSTRACT

A combined experimental and theoretical study on molecular dynamics of 4-Benzyloxy 3 -Methoxybenzadehyde has been undertaken. All the quantum computations in this study were carried out using B3LYP functional and 6-311++G (d, p) basis set. The conformational analysis was done using Potential energy surface scan by varying a suitable dihedral angle and the conformer of the molecule with the minimum energy was found out. The vibrational characterization of the molecule is carried out using FT-IR and FT-Raman spectra recorded in the range of 4000 – 400 cm^{-1}. All the normal modes were assigned based on the potential energy distribution value corresponding to that mode. The molecular orbital analysis of the molecule was done through NBO, HOMO – LUMO and UV visible spectral analysis. The prominent donor and acceptor orbitals were identified through stabilization energy; the types of interaction were simulated through H–L contribution. The atomic charges are predicted theoretically by Mullikan and Natural methods, and are used to analyze the NMR chemical shift of the carbon and Hydrogen atoms of the molecule. The ^{1}H and ^{13}C NMR chemical shifts are calculated using the Gauge-Including Atomic Orbital (GIAO) method with B3LYP/6-311++G (d, p) method.

Keywords:— *4-Methoxy biphenyl; DFT; vibrational spectra; chemical shifts; Molecular docking; NBO.*

I. INTRODUCTION

4-hydroxy-3-methoxybenzaldehyde is also known as Vanillin which is the primary chemical component of the extract of vanilla bean. Natural vanilla extract is a mixture of several hundred compounds in addition to vanillin. Vanillin ($C_8H_8O_3$) is a naturally occurring phenolic aldehyde that occurs both as free vanillin and as a fragment of some macromolecules [1]. It is used widely as a flavoring additive in beverages, cooking, and as an aromatic additive in candles, incense, potpourri, fragrances, perfumes, and air fresheners.

Because of the high cost of authentic vanilla extracts, artificial vanilla flavorings

are also used which contain ethyl vanillin dissolved in alcohol, propylene glycol, and glycerin. Some manufacturers have adulterated vanilla extracts with coumarin in order to increase the vanilla flavor perception. Coumarin, a phytochemical found in many plant species, has a sweet herbaceous odor and has been used in food, tobacco and cosmetics as a flavoring and fragrance enhancer. It may be isolated from the vanilla bean, and is often obtained as a byproduct of the pulp and paper industry by the oxidative breakdown of lignin [2].

Vanillin is found in several food stuffs [3, 4, 5] and its presence in certain type of corks seems to be essential for the antioxidant activity in some wines [6]. Additionally, vanillin shows non-linear optical propertie with higher second harmonic generatio efficiency, possessing great potential application in optical device. Recently, Vanillin was shown to suppress the invasion and migration of cancer cells in vitro, and to inhibit the metastasis of mouse breast cancer cells [7].

In addition, vanillin or its derivatives was shown to inhibit the activity of DNA-dependent protein kinase catalytic subunit (DNA-PKcs), a key component involving in the non-homologous end joining (NHEJ) pathway of DNA double-strand breaks, and sensitize cancer cells to genotoxic agents [8, 9, 10].

Vanillin exists as an acid in solution. Exposure to high levels of vanillin can be irritating to eyes and mucous membranes of the respiratory tract. Vanillin is classified as generally recognized as safe (GRAS) by the Flavor and Extract Manufacturers Association (FEMA). The wide application of Vanillin impelled this study in order to understand the complete dynamics of the molecule through spectroscopic and computational analysis, as no such report is available in the literature survey.

II. METHODS

Experimental Details

The compound under investigation 4-Benzyloxy 3-Methoxybenzadehyde was purchased in the powder form from Sigma-Aldrich chemicals company, USA. The FT-IR spectrum of the component was recorded using a Bruker IFS 66 V spectrometer using KBr pellet technique in the range of 4000-400 cm^{-1}. The FT-Raman spectrum was also recorded in the same instrument in the same region using Nd-YAG laser at 1064 nm. The NMR chemical shift was recorded di-methyl sulphoxide (DMSO) solvent in the range of 20-200 ppm with the scanning interval of 20 ppm and UV-Visible spectrum was recorded in the range of 200-400 nm, with the scanning interval of 0.2 nm, using the UV-1700 series instrument.

Computational Details

The molecular geometry of the 4-Benzyloxy 3-Methoxybenzadehyde is calculating by Density Functional Theory (DFT) and calculating the electronic structures of molecule by basic sets B3LYP 6-311++G (d, p) was augmented by a ‘d’ polarization function for heavy atoms and ‘p’ polarization for hydrogen atoms. All the quantum chemical computations in the present work are performed using the Gaussian 09 software programs [11] on a Pentium IV/3.02GHz personal computer. Geometrical parameters and vibrational wave numbers were computed by optimizing the geometry of the molecule using the B3LYP methods with 6-311++G (d, p) as a basic set. The vibrational frequency assignments were calculated by the total energy distribution (TED) method using the Vibrational Energy Distribution Analysis (WEDA-4) program the optimized

geometry of the molecule 4-Benzyloxy 3-Methoxybenzadehyde was further used to Complete a Natural Bond Orbital (NBO) analysis using NBO version 3.1 which is implemented in the Gaussian 09W package. The NMR chemical shifts of the were also 4 -Benzyloxy 3-Methoxybenzadehyde calculated using the Gauge Independent Atomic Orbital's (GIAO) method with the B3LYP/6-311++G (d, p) functional method. The NMR chemical shift ^{1}H and ^{13}C was carried out by GIAO method in B3LYP method with 6-311G++ (d, p). The energy distribution from HOMO to LUMO and Mullikan charges dipole moment of the title molecule are also computed using B3LYP method with same basis set.

III. Result and Discussion

Conformational Analysis

Different orientation of the molecule, using the dihedral angle 25H-24C-23O-13C and their corresponding energies are calculated using potential energy surface scan method and plotted against the scan coordinates, the resulting curve is shown in Figure 1. It was carried out using semi empirical method PM6 because it yields reliable results and consume less time compared to DFT methods [12]. It clearly shows that there are two minima at -180º and - 65º with 0.0847 Hartree energy. Hence these conformers both of them are structurally identical, serve as the most stable conformer of the compound. The maximum energy is observed for the conformer at 0º and -128º with energy value -0.0835 Hartree, which is the least stable or most unstable conformer of the compound. The most stable conformer of the compound shown in Figure 2 is used for all the computational analysis in this study.

Structural Analysis

The structural parameters bond length, bond angle and dihedral angles were obtained for the most stable conformer of the compound using B3LPYfunctional and 6-311++ G(d, p) basic set and the values are presented in Table.1.

The CC single bond lengths of the aromatic rings are mostly found to 1.39 Å, one CC bond length in each ring is 1.38 Å and one is 1.40 Å, these are in agreement with pure benzene values 1.38 Å to 1.39 Å [13]. This is surprising results, though there are three substitutional groups in the molecules, the CC bond lengths of phenyl rings are remain undisturbed. This means the electronic conjugation within the rings is identical and uninfluenced by the methoxy and aldehide substitutions. The CC bond length of aliphatic chains C4-C29 and C15-C28 bond get the values 1.502 & 1.478 Å respectively. These bonds are CC single bonds which are expected around 1.45 Å, but these values are higher than the expected region. This may be due to the presences of oxygen atom both in methoxy and aldehide group, which might have increased the positive charges among the carbon atoms, resulting in repulsion between them. The variation among them is clearly due to the difference between the constituent of them.

In the case of CH bond lengths, it is observed that all the CH bond lengths in both phenyl rings show the same value of 1.08 Å, which is in agreement the experiment value [14]. This shows that these bond lengths are also not affected by the influence of substitutional groups. The CH bonds in the methoxy groups are found to be 1.09 Å whereas in aldehide group it is 1.11 Å, which subtly indicate the difference in electronic distribution in these groups.

In the present molecule there are five CO bond lengths, the bonds C12-O21and C13-

O23 which are attached to benzene ring have value 1.37Å. The bonds O21-29C and O23-C24 which are connected to aliphatic carbon have values 1.45 and 1.43 respectively, which are rather pure CO single bond values whereas the 1.37 Å values in the former case are neither single bonded nor double bonded CO. This indicates a fact that the electronic conjugation among the CC bonds within the ring extents to even CO bonds, which are attached to the rings, resulting in bonds having length in between single and double bonds. The O22-C28 bond in the aldehide group is found to have length 1.211 Å, indicating it is a double bond.

The bond angle of the carbon atom in the benzene ring is around 120° due to sp2 hybridization [15]. In this title molecule, all the CCC bond angles C2-C3-C4, C4-C5-C6, C1-C6-C5, C13-C14-C15, C12-C17-C16, C3-C4-C29, C5-C4-C29 and C16-C15-C28 are in the range of 120º, except bond angles which are centered around 15C, 12C, 13C and 4C are found to have values in between 118-119°. All these atoms are attached to the substitutional groups, hence the hybridization are changed by the redistribution of the charges around them. The 120º angle is expected for all C-C-H single bonds also, but variation in the bond angles 119º to 120º is observed for these C-C-H single bonds also. The angles C15-C28 -H2 and C4-C29-H30 show the values 109º and 111º which clearly shows that the second benzene ring is influenced on the methoxy attachment. The CCO bond angle C15-C28-O22 value is very high (125º) compared to the reference value. The C4-C29-O22 bond angle value is very less 108.6º, which shows the hybridization is changed to sp3 due to the combination with oxygen atom.

Mullikan and Natural atomic charge analysis

The atomic charges exhibit direct influence on the dipole moment, molecular polarization, electronic structure, molecular reactivity, vibrational frequency of the system and so on. It also determines the NMR chemical shift and many more properties of the molecular system. The charges on the atoms of the molecule 4-Benzyloxy-3-methoxybenzaldehyde was computed by both Mullikan population analysis (MPA) method and Natural atomic charge (NAC) method using B3LYP functional with 6-311++G (d, p) basis set , and are presented in Table .2 and graphically in Figure 3.

The carbon atoms in both benzene rings are expected to be equally negative [16], as they share the electrons within the ring equally due to conjugation. The C4 carbon atom which is attached to methoxy group is predicted with maximum positive chare 0.828 in MPA method whereas almost neutral in NCA method. Whereas the C12 atom which is attached to the same methoxy group from other benzene ring is found to be highly negative (-0.705) and positive (0.283) in NCA method. C13 is the atom in second benzene ring where another methoxy group is attached is found to be positive in both the methods (0.406 & 0.282). C15 is the atom where the aldehide group is attached is found to be relatively highly positive in MPA (0.556) and negative in NCA (-0.152). Carbon C29 which is in methoxy group gets maximum negative value (-0.953) in MPA and almost neutral in NCA (-0.023). The difference in the charge predicted by two methods indicate the difference in the logic used in the calculation, however this can be verified which is valid by comparing with the experimental NMR chemical shift value.

The entire hydrogen atoms in the title molecule are predicted positive below 0.25 in

both the methods. There are three oxygen atoms O21, O22, O23, among them only O21 is predicted positive in MPA while the other two get only negative values. O21is the atom in the methoxy group held between the two benzene rings, is believed to donate the both the electrons to C29 making it highly negative in the molecule.

NMR Analysis

The chemical shift for the H and C atoms of the molecule are computed by GIAO method using B3LYP functional with 6-311++ G (2d, p) basis set for optimized geometry of the compound. The computed values in gas and solvent phase along with the experimental values in solvent phase are presented in Table 3, and the spectra of the same are shown in Figure 3 & 4.

The aromatic carbon atoms are expected to have shifts in the range of 120-130 ppm [17]. In the title molecule, the chemical shifts of the aromatic carbon atoms are in expected range 128-130 ppm, except for 4C (150 ppm), 12C (150 ppm), 13C (153 ppm), 15C(136 ppm), 24 C (56 ppm), 28 C (190 ppm) and 29 C (77 ppm) experimentally. The 4C carbon atom which is attached to methoxy group is predicted with maximum positive chare 0.828 in MPA method whereas almost neutral in NCA method. The NMR shift thus supports the NCA prediction. Similarly, the C12 atom which is attached to the same methoxy group from other benzene ring is found to be highly negative (-0.705) and positive (0.283) in NCA method, this also is found to have the same chemical shift as that of 4C, thus the prediction again by MPA cannot be correct, only the NCA prediction holds good. C13 is the atom in second benzene ring where another methoxy group is attached is found to be positive in both the methods (0.406 & 0.282), this is also found to have same shift 153 ppm, which again confirm the validity of the NCA prediction. 15C is the atom where the aldehide group is attached is found to be relatively highly positive in MPA (0.556) and negative in NCA (-0.152), the shift for 15C is 136, this is almost equivalent to unaffected carbon atom in benzene ring, thus the negative charge predicted by NCA is reasonable.

Carbon C29 which is in methoxy group gets maximum negative value (-0.953) in MPA and almost neutral in NCA (-0.023). The chemical shift 29C is 77 ppm, which is actually an aliphatic carbon whose value here is found to be enhanced from 30 ppm. This is naturally due to the presence of oxygen in this group, thus the prediction of charge by NCA method is proven to be correct. C28 is present within the aldehide group, this is predicted slightly negative (-0.174) in MPA and highly positive (0.418) in NCA. This is found to have the maximum chemical shift in the compound 190 ppm , which is possible only when it is extremely positive as predicted by NCA.

The chemical shifts of the hydrogen atoms are found almost below 7.5 ppm, which shows that chemical environment of the hydrogen atoms in the benzene rings are not affected by substitutional groups. There is appreciable difference observed in the chemical shifts of 32H (9.8 ppm) which is present in the aldehide group, this is naturally due to the presence of O atom in this group. The chemical shift of 30H, 31H and 27H are found to be around 5 ppm, these are present in the methoxy group, but for the presence of O in these groups, their values would be around 3 ppm, like in methyl group.

Vibrational Analysis

The title molecule under investigation has 35 numbers of atoms and therefore 99 normal modes of fundamental vibrations. Most of them are found active either in IR and Raman, except the last few that are not recorded as they fall in the range 400 to 100 cm^{-1}. The

assignments of all the fundamentals have been made on the basis of PED values along with the computed values. The assignments are discussed in comparison with the counter parts available in the literature on the structurally similar molecules. The calculated wave numbers are found slightly higher than the observed values for the majority the normal modes. Two factors may be responsible for the discrepancies between the experimental and computed wave numbers; the first is caused by the unpredictable electronic distribution among the different bonds in the molecule and the second reason is the anharmonic nature of the vibrations which cannot be accounted completely by theory. Scaling strategies were used to bring computed wave numbers to coincide with observed values. In this study, the scaling factors used is 0.9026 as advised by the earlier work [18], All the computed and experimental wave numbers along with the assignments and PED values are presented in Table.4. The Experimental FTIR and FT Raman spectral are shown in Figure 5 & 6 respectively.

C-H vibrations

In the aromatic compounds, the C-H stretching normally occurs in the region of 3100-3000 cm^{-1} [19]. For the title molecule, there are eight CH stretching vibrations of benzene rings, which are observed at 3090, 3080, 3072, 3065, 3062, 3060, 3058, 3034 cm^{-1}, all these are found completely within the range which shows they are not affected by the substitutional groups, as predicted in the earlier analyses. There are six CH bonds in the aliphatic groups; five in methoxy and one in aldehide groups respectively. These are found at 3013, 2990, 2950, 2921, 2840 2763cm^{-1}. Some values are pushed up and some are pulled down, these are impact observed as due to the influence of O atoms in the methoxy and aldehide groups on the CH stretching vibrations. Theoretically, the CH stretching vibrations are observed at 3094 -2790 cm^{-1} respectively. The entire aromatic C-H stretch mode is pure stretching modes as it is evident from PED values.

Normally the strongest absorptions for in-plane and out of plane bending CH vibrations occur in the region 1300-1000 cm^{-1} and 1000-750 cm^{-1} respectively [20,21]. The distinction between the aromatic and aliphatic among bending vibrations will not be there. In the title compound, the in-plane bending vibrations are found at 1196, 1157, 1133, 1130, 1030 and 990 cm^{-1} at IR region and 1209, 1189, 1168, 1140,1090, 1020 and 996 cm^{-1} at FT- Raman. Theoretically, these vibrations are observed in the range 1205 to 985 cm^{-1}. These values show entire vibrations are observed at the middle of the expected region, hence there is no visible influence of O atoms in the CH bending modes.

C-C vibrations

The ring stretching vibrations are very much important in the spectrum of benzene and its derivatives. The bands between 1600 -1400 cm^{-1} in are usually assigned to benzene CC modes, particularly 1600-1500 cm^{-1} to C=C [22] and 1500-1400 cm^{-1} to C-C modes[23], even though no such clear distinction occurs as C=C and C-C within the rings due to electronic conjugation. However, the vibrations can be taken to be closer to double bond and single bond CC, as the electronic distribution is not entirely uniform among these bonds. In the present compound, six C=C stretching vibrations can be assigned to 1676, 1584, 1570, 1550, 1484, 1464 cm^{-1} and the six C-C to and 1463, 1446, 1424, 1440, 1399, 1370 cm^{-1} within the rings. There are two C-C bonds outside the ring which are assigned at 1347 and 1318 cm^{-1} respectively. Theoretically, the CC stretching vibrations are observed at 1592 - 1313 cm^{-1} respectively. All these values are exactly as they should be except a few values which are found above and below the expected ranges.

C-O vibrations

As per the previous literatures, the C=O stretch of carboxylic acids is identical to the C=O stretch in ketones, which is expected in the region 1740–1660 cm^{-1} [24] and C-O single bond is expected in the region 1220-970 cm^{-1}. In the present molecule, the C=O stretching band is observed at FT-IR 1727 cm^{-1}. Theoretical wave number of this mode is 1705cm^{-1}. This values lie at the higher end of the expected range. It seems the CO modes in this molecule are boosted by sharing energy with CH modes. The C=O in-plane bending mode based on the PED contribution is assigned to 1157 cm^{-1}, though it is expected to be with in-plane bending modes of C-O, whose in-plane and out of plane bending modes are expected in the range 625±70 cm^{-1} and 540±80 cm^{-1} respectively. C-O stretching are observed at 1305, 1289, 1263 and 1236 cm^{-1} .

Theoretically, the C-O stretching vibrations are observed at 1298 - 1232 cm-1 respectively. Comparing with expected region from literature, they are very much at the top end, which confirms all these modes are enhanced due to sharing the electrons from CH bonds. The in-plane bending vibrations of CO are assigned at 977, 968, 958, 956 and 948 cm-1 (FT-Raman) frequencies. The CO out of plane bending vibrations is assigned to the band at 560, 485 and 422 cm-1 in FTIR and at 588 cm-1 in FT-Raman.

NBO Analysis

The Natural bond analysis (NBO) is most important method for studying the various possible donors and acceptors in the molecule with their occupancy value in each position. Similarly the various possible transitions among these donors and acceptors, inter and intra molecular interactions can also be studied using this method. The NBO occupied orbital is Lewis -type (bond or lone pair) and unoccupied orbital is non-Lewis type (anti-bond or Rydberg). NBO analysis was performed on the title molecule at the B3LYP/6-311+G (d,p) basis set level. The Fock matrix was elucidated for the donor-acceptor interactions, for which the stabilization energy $E^{(2)}$ were determined [25] using the relation:

$$E_2 = \Delta E_{ij} = q_i \frac{F(i,j)^2}{E_i - E_j}$$

Where q_i is the donor orbital occupancy, ε_i and ε_j diagonal elements and *F(i,j)* is the off diagonal elements of Fock matrix. Higher the stabilization energy of a transition, higher is the probability for that transition to take place. Based on these stabilization energy values, the most probable transitions in this molecule are C13-C14 to C12-C17(π -π*, 23.2 Kcal/mol), O22 to C 28-H32 (n-π *, 22.97 Kcal/mol), C15- C16 to C13 - C14 (π -π*, 22.61Kcal/mol), C12-C17 to C15-C16 (π -π*, 21.42 Kcal/mol), C12-C17 to C15-C16 (π -π*, 21.42Kcal/mol), C2-C3 to C4-C5 (π -π*, 21.09Kcal/mol) C2-C3 to C1-C6 (π -π *, 20.31Kcal/mol), C4-C5 to C2-C3 (π -π*, 20.23Kcal/mol), C4-C5 to C1-C6 (π -π*, 20.04Kcal/mol), C1-C6 to C4-C5 (π -π*, 20.02Kcal/mol). All these π -π* transitions are usual transitions which take place within the benzene ring, but the only n -π* transition which appeared in the list is due to the aldehide group, which means no important transition is available in methoxy groups. However some of the transitions may not be favoured by the selections rules, so they may not be visible in the experimental Uv-Vis spectrum. The lines which appear in the spectrum can also predicted theoretically using the HOMO – LUMO contributions, which is discussed in the following section.

UV-VISIBLE Analysis

Ultraviolet spectral analysis of the title molecule 4-Benzyloxy 3-Methoxybenzadehyde was done both theoretically and experimentally. The theoretical computation was done using TD-SCF functional along with B3LYP/6-311++G(d,p) combination. The calculated absorption maximum wavelengths λ_m, oscillator strength and excitation energy for different possible electronic transitions are presented in Table 6. Among these parameters the oscillator strength indicates the intensity of the peak in the spectrum or the transitions which are favoured by the selection rules.

In this case, UV analysis was carried out for the top ten transitions based on the stabilization energy values in gas phase and in ethanol phase in which the experimental spectrum was recorded. The energy gaps in solvent phase for the ten transitions are found to be 3.830, 4.299, 4.531, 4.670, 4.729, 4.839, 5.299, 5.530, 5.602 and 5.656 eV respectively. The respective oscillator strength, which theoretically predict the intensity of the bands are 0.0004, 0.2902, 0.1427, 0.0105, 0.1346, 0.0476, 0.0018, 0.0954, 0.0395 and 0.1469 respectively. The calculated absorption maximum values are 323, 288, 273, 265, 262, 256, 233, 224, 221, 219 nm. As can be seen from the oscillator strength, only the second transition in the order has the maximum oscillator strength among them and also the maximum HOMO- LUMO contribution, which clearly indicates that second transition will have the maximum intensity at wavelength 288nm among the appeared peaks. There are possibility for peaks at 219, 262, 273 nm also with relatively less intensity. The experimental spectrum shows three prominent peaks at 215, 277 and 310 nm, of which the peak at 277 nm is due to the electronic transition O22 to C 28-H32 (n -π*, 22.97 Kcal/mol), Whose HOMO-LUMO contribution in the highest, 76%, predicted at 288 nm theoretically. The other two bands are less probable theoretically but appeared in the experimental spectrum.

In gas phase, the energy gaps for these ten transitions are found to be 3.696, 4.429, 4.679, 4.837, 4.873, 4.980, 5.291, 5.450, 5.498 and 5.709 eV respectively. The respective oscillator strengths are 0.0002, 0.3089, 0.1539, 0.0188, 0.0761, 0.0161, 0.0010, 0.0312, 0.0049 and 0.2693 respectively. The calculated absorption maximum values corresponding to these are 335, 279, 264, 256, 254, 248, 234, 227, 225, and 217nm respectively. The comparison of these values with values in solvent phase indicate that the oscillator strengths and absorption wavelengths are altered due to the change in phase, that shows the impact of solvent on electronic transitions.

HOMO – LUMO Analysis

Frontier molecular orbital (FMO) theory explains the stability of a molecular orbital's, the distribution of charges at various ground and virtual states and the energy gap between them [26]. The highest occupied molecular orbital (HOMO) and lowest unoccupied molecular orbital (LUMO) are the important molecular orbital's in FMO. These orbitals play a major role in governing many chemical reactions and determining electronic band gaps in solids; they are also responsible for the formation of many charge-transfer complexes. The energy gap between HOMO and LUMO determines molecular electrical transport properties, chemical reactivity, electrophilic index, hardness and softness of the molecule.

The mapping and energies HOMO and LUMO are computed with B3LYP functional with 6-311++ G (d, p) basis set and the same is presented in Figure 9 and

Table 7 respectively along with other related parameters.

According to the computed results, 4-benzoyloxy 3-methoxybenzaldehyde contains 50 occupied molecular orbital's and 50 unoccupied molecular orbital's. The calculated average energy of the HOMO is -0.256 eV and that of LUMO is -0.080 eV. The energy gap between them for optimized structure is -0.176eV, which shows the possibility of flow of energy form HOMO to LUMO. The electronegativity is a measure of attraction of an atom for electrons in a covalent bond which has been found to be 0.168 eV. The global hardness is a measure the resistance of an atom or a group of atoms to receive electrons and is equal to reciprocal of global hardness and it is found to be 0.088 eV. The global softness describes the capacity of an atom or a group of atoms to receive electrons and is equal to reciprocal of global hardness and it is found to be 0.352eV. The electrophilicity index is a measure of lowering of total energy due to the maximal electron flow between the donors and the acceptors and it is found to be 0.161 eV. The dipole moment transitions value is 4.4276 (debye).

Molecular Electrostatic Potential (MEP) analysis

A MEP surface is an electron density isosurface mapped with an electrostatic potential surface. The MEP surface for the compound can be used to determine their sizes, shapes, charge densities and reactive sites. Different values of electrostatic potential at the surfaces are represented by different colours; red represents regions of most negative electrostatic potential, blue represents regions of most positive electrostatic potential and green represents regions close to zero electrostatic potential. The electrostatic potential increases in the order: Red < Orange < Yellow < Green < Blue [27]. The colour code of these maps in the range between -5.268 e-2 (deepest red) and 5.268 e-2 (deepest blue)

The negative (red and yellow) regions of the MEP surfaces are related to electrophilic reactivity and the positive (blue) regions to nucleophilic reactivity. The negative region of the MEP is mainly surrounded over the oxygen atom O of aldehide group and slightly (yellow region) over the methoxy group in between the two benzene rings, indicating the nucleophilic region. The positive region is localized over the hydrogen atoms in both benzene rings, showing the possible sites for electrophilic attacks.

Docking Analysis

The docking of the present molecule with suitable protein was carried using BAITOC an online tool and Autodock 4 software package, the output of which is shown in Table. 8. For docking study, high resolution fine crystal structure of Mycobacterium tuberculosis thymidylate kinase complexed with thymidine-5'-diphosphate (PDB ID: 1GTV) is used as a receptor. The protein structures were prepared with the help of AutoDock Tools Graphical user interface. Polar hydrogen was added to the protein, atomic charges were calculated by kollman method. The Lamarckian genetic algorithm (LGA) was utilized for molecular docking calculation to be used in AutoDock 4.0 software package. The ligand PDB molecule was used in optimized molecular geometry. The active site of the protein were located with the use of grid size 80 Å × 80 Å × 80 Å using Autogrid. The Discover studio Visualized 4.0 is utilized for view of 2D and 3D best binding sites.

The molecule was found to dock with the targeted the protein at two different places, with the formation of hydrogen bonds from the oxygen atoms, one is from the aldehide group (CYS 79) and another is from the first methoxy group kept (GLN 38) between

two benzene groups. The best lowest energy docked position of the molecule with target protein is illustrated in Fig. 11 , the binding energy at this position is found to be -5.79 Kcal/mol. In pictorial the Yellow dotted lined denote the formation of hydrogen bond of ligand with target proteins. The hydrogen bond formed at the aldehide site is found to be longer (2.9 Å) than that formed at methoxy group (2.2 Å) which implies the binding at the aldehide sites is stronger than that at the methoxy site.

IV. FIGURES AND TABLES

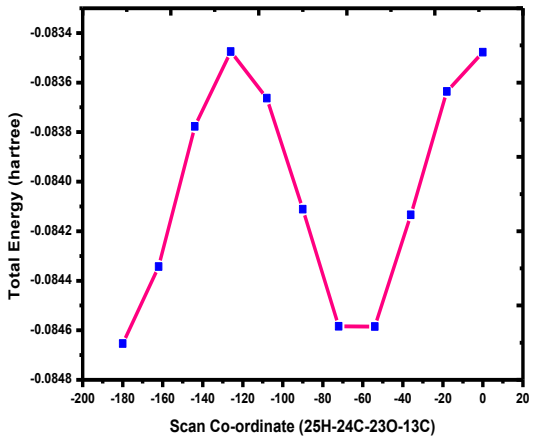

Figure 1: Conformational Energy surface scan of 4-Benzyloxy 3-Methoxybenzadehyde

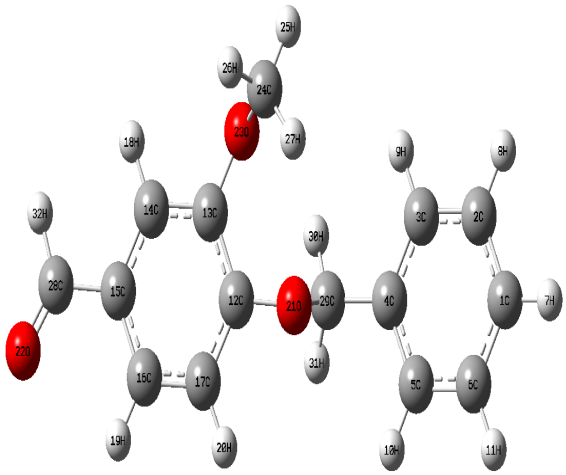

Figure 2: Molecule of 4-Benzyloxy 3-Methoxybenzadehyde

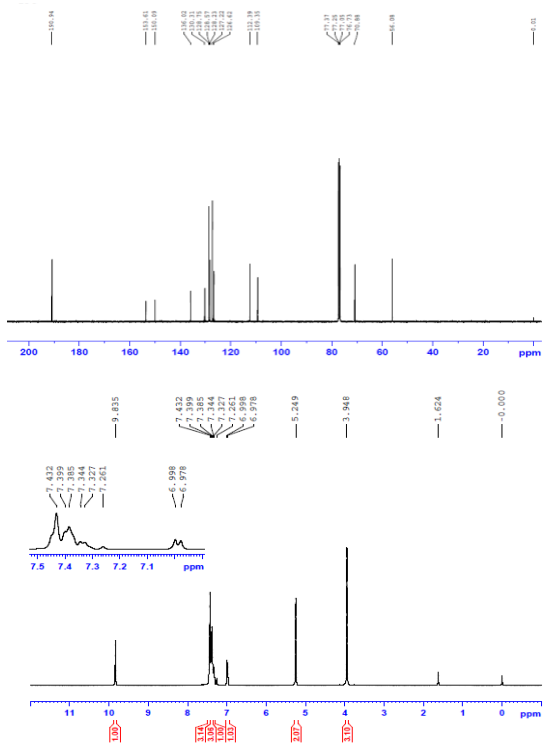

Figure 4: Experimental ^{1}H NMR of 4-Benzyloxy 3-Methoxybenzadehyde

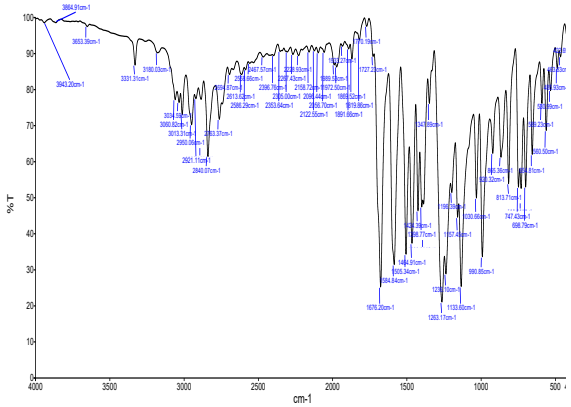

Figure 5: FT-IR Experimental Spectrum of 4-Benzyloxy 3-Methoxy Benzaldehyde

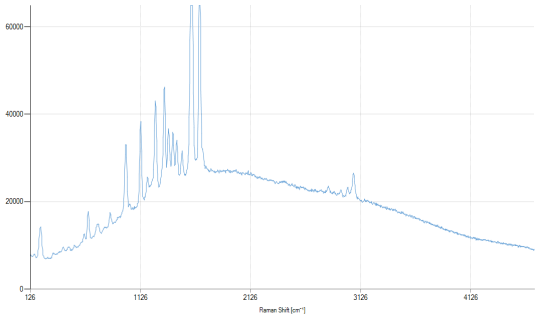

Figure 6: FT-Raman- Experimental Spectrum of 4-Benzyloxy 3-Methoxybenzadehyde

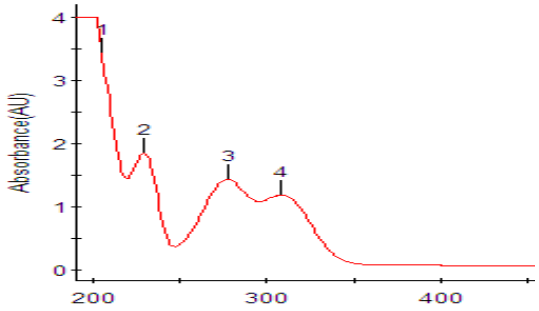

Figure 7: and 8 UV-Visible experimental and theoretical spectrum of 4-benziloxy 3-methoxy benzaldehyde

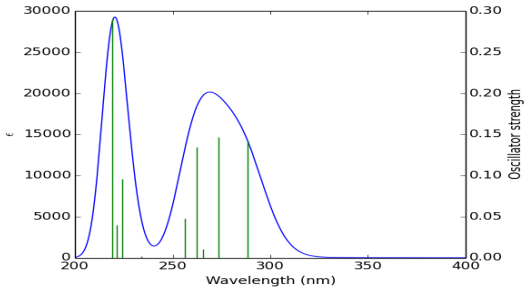

Figure 8: UV-Visible experimental and theoretical spectrum of 4-benziloxy 3-methoxy benzaldehyde

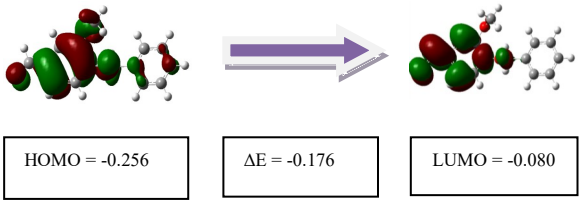

Figure 9: Frontier molecular orbital of 4-benziloxy 3-methoxybenzaldehyde

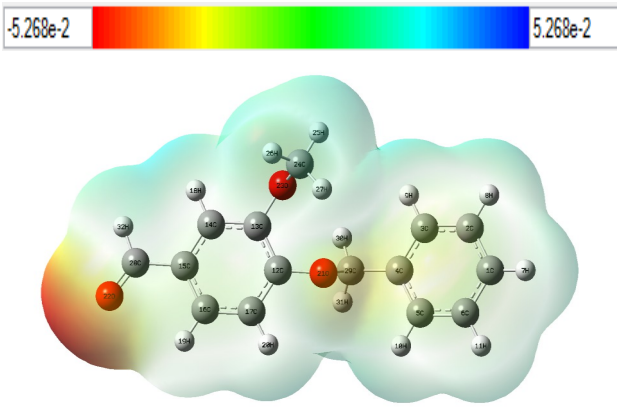

Figure 10: Molecular Electrostatic Potential (MEP) analysis 4-Benzyloxy-3-methoxybenzadehyde

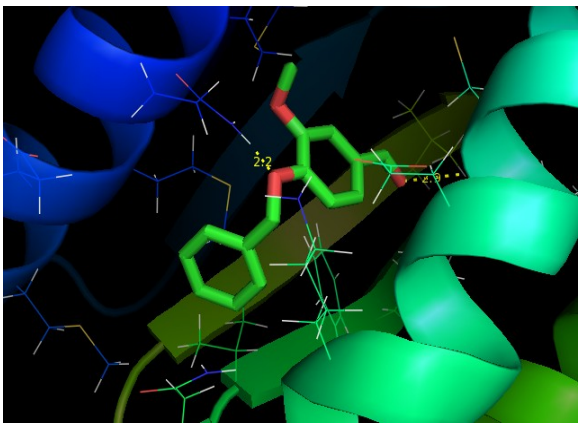

Figure 11: 3D view of the docking sites of the molecule with target Protein

Table 1: Optimized Geometrical parameter for 4-Benzyloxy 3-Methoxybenzadehyde

Bond Length (Å)	B3LYP 6-311++G (d,p)	XRD	Bond Angle (°)	B3LYP 6-311++G (d,p)	XRD
Benzene ring (CC)			Benzene ring (CCC)		
C1-C2	1.393	1.38	C1-C2-C3	119.9	119.8
C2-C3	1.394	1.39	C2-C3-C4	120.6	120.5
C3-C4	1.397	1.39	C3-C4-C5	118.9	119.1
C4-C5	1.398	1.39	C4-C5-C6	120.5	120.6
C5-C6	1.391	1.39	C1-C6-C5	120.0	120.1
C6-C1	1.395	1.40	C2-C1-C6	119.8	119.9
C12-C13	1.407	1.42	C12-C13-C14	119.3	119.8
C13-C14	1.390	1.38	C13-C14-C15	120.7	120.5
C14-C15	1.399	1.39	C14-C15-C16	119.6	119.7
C15-C16	1.400	1.40	C12-C17-C16	120.5	120.2
C16-C17	1.386	1.39	C15-C16-C17	119.8	120.3
C12-C17	1.398	1.39	C13-C12-C17	119.7	119.6

Out of ring (CC)			Out of ring(CCC)		
C4-C29	1.502	1.50	C3-C4-C29	120.5	120.5
C15-C28	1.478	1.47	C5-C4-C29	120.4	120.4
(CO) Ring			C14-C15-C28	119.3	119.8
C12-O21	1.370	1.37	C16-C15-C28	120.9	120.3
C13-O23	1.374	1.35	(CCO) Ring		
O21-29C	1.456	1.45	C12-C13-O23	121.0	122.1
O22-C28	1.211	1.21	C13-C12-O21	120.8	120.9
O23-C24	1.437	1.42	C17-C12-O21	119.2	124.9
(CH) Ring			C4-C29-O21	108.6	
C1-H7	1.084	1.08	C15-C28-O22	125.0	125.2
C2-H8	1.084	1.08	C14-C13-O23	119.5	125.1
C5-H10	1.084	1.08	(CCH)Ring		
C6-H11	1.084	1.08	C1-C2-H8	120.1	120.1
C16-H19	1.083	1.08	C2-C3-H9	119.8	119.9
C17-H20	1.083	1.08	C2-C1-H7	120.1	120.1
C24-H25	1.089	1.09	C3-C2-H8	119.9	119.6
C24-H26	1.094	1.09	C4-C3-H9	119.4	119.5
C24-H27	1.092	1.09	C6-C1-H7	120.0	120.1
C28-H32	1.110	1.11	C4-C5-H10	119.5	119.6
C29-H30	1.092	1.09	C6-C5-H10	119.9	120.0
C29-H31	1.095	1.09	C1-C6-H11	120.0	120.0
C3-H9	1.085	1.08	C5-C6-H11	120.0	120.0
C14-H18	1.085	1.08	C13-C14-H18	118.5	121.6
			C15-C14-H18	120.7	117.8
			C15-C16-H19	118.9	119.9
			C17-C16-H19	121.1	119.7
			C12-C17-H20	118.1	119.7
			C16-C17-H20	121.2	119.6
			C4-C29-H30	111.0	111.0
			C4-C29-H31	111.0	111.0
			C15-C28-H32	114.5	114.3
			(COC) Ring		
			C12-O21-C29	115.0	119.3
			C13-O23-C24	114.9	118.0
			(HCH) Ring		
			H25-C24-H26	109.4	109.4
			H25-C24-H27	109.9	109.5
			H26-C24-H27	109.9	109.5
			H30-C29-H31	108.9	108.2
			(OCH) Ring		
			O23-C24-H25	106.0	105.6
			O23-C24-H26	110.3	111.3
			O23-C24-H27	111.0	111.3
			O22-C28-H32	120.4	120.3
			O21-29C-H30	109.2	109.5
			O21-C29-H31	107.8	109.5

Table 2 : Charges of 4-Benzyloxy-3-methoxybenzaldehyde with B3LYP/6-311++G (d,p) basis set.

Atoms	B3LYP/6-311++G(d,p)	
	Mullikan Charge	Natural Charge
C1	-0.186	-0.195
C2	-0.296	-0.194
C3	-0.079	-0.188
C4	0.828	-0.052
C5	-0.258	-0.187
C6	-0.288	-0.193
H7	0.156	0.203
H8	0.169	0.202
H9	0.151	0.204
H10	0.142	0.202
H11	0.171	0.203
C12	-0.705	0.283
C13	0.406	0.282
C14	-0.482	-0.172
C15	0.556	-0.152
C16	-0.156	-0.145
C17	0.081	-0.221
H18	0.202	0.223
H19	0.211	0.230
H20	0.199	0.220
O21	0.021	-0.580
O22	-0.231	-0.542
O23	-0.111	-0.539
C24	-0.515	-0.867
H25	0.248	0.343
H26	0.167	0.371
H27	0.229	0.386
C28	-0.174	0.418
C29	-0.953	-0.023
H30	0.177	0.178
H31	0.153	0.170
H32	0.162	0.131

Table 3: Calculated ^{1}H and ^{13}C NMR Chemical shifts (ppm) 4-Benzyloxy-3-Methoxybenzadehyde

Atom	Gas B3LYP/6311++G(d,p) GIAO (ppm)	$CDCl_3$ B3LYP/6-311++G(2d,p)GIAO (ppm)	Experimental
1C	133.3	133.3	128.7
2C	133.0	133.6	128.7
3C	134.9	135.3	130.3
4C	142.9	143.0	150.9
5C	135.9	135.8	130.3
6C	133.4	133.6	128.7
12C	166.4	167.2	150.0
13C	161.3	161.6	153.6
14C	134.7	135.9	130.3
15C	139.6	139.4	136.0
16C	129.1	128.7	128.5
17C	129.4	129.8	128.7
24C	61.7	62.10	56.08
28C	193.4	196.4	190.8
29C	79.9	79.8	77.3
7H	7.56	7.67	7.43
8H	7.49	7.64	7.39
9H	7.72	7.85	7.39
10H	7.78	7.94	7.43
11H	7.63	7.74	7.38
18H	7.53	7.71	7.34
19H	8.60	8.06	7.43
20H	7.40	7.52	7.43
25H	3.94	4.05	3.94
26H	3.34	3.44	3.94
27H	4.37	4.34	5.21
30H	5.31	5.34	5.21
31H	4.60	4.72	3.94
32H	10.17	10.15	9.83

Table 4 : Observed method DFT/B3LYP with 6-311++G(d, p) level calculated vibrational frequencies of 4-Benzyloxy-3-Methoxybenzaldihyde

Experimental frequency cm-1		B3LYP 6-311++G(d, p)		Assignment	VEDA %
FT-IR	FT-RAMAN	Un scaled (cm^{-1})	Scaled (cm^{-1})		
	3090	3199	3094	ν CH	ν CH 99
	3080	3190	3084	ν CH	ν CH 91
	3072	3183	3078	ν CH	ν CH 88
3065		3180	3075	ν CH	ν CH 70
3062		3171	3067	ν CH	ν CH 55
3060		3171	3066	ν CH	ν CH 38
	3058	3163	3058	ν CH	ν CH 39
3034		3159	3054	ν CH	ν CH 79
3013		3133	3029	ν CH	ν CH 96
	2990	3099	2988 .988	ν CH	ν CH 91
2950		3087	2985 .439	ν CH	ν CH 95
2921		3020	2921	ν CH	ν CH 18
2840		3018	2918	ν CH	ν CH 72
2763		2885	2790	ν CH	ν CH 78
1727		1763	1705	ν C=O	ν CO 88
1676		1646	1592	ν CC	ν CC 14
1584		1635	1581	ν CC	ν CC 58
1570		1626	1572 59	ν CC	ν CC 19
	1550	1599	1546	ν CC	ν CC 68
	1481	1523	1473	ν CC	ν CC 89
1464		1517	1467	ν CC	ν CC 58
	1463	1507	1458	ν CC	ν CC 58 + β CCH 10
	1446	1490	1441	ν CC	γ CHO 32+ β CCH 15
	1440	1484	1435	ν CC	ν CC 32+β CHO 28
1424		1480	1431	ν CC	ν CC 33+ ν CHO 20
	1399	1443	1395	ν CC	ν CC 10
	1370	1410	1364	ν CC	ν CC 11
1347		1395	1349	ν CC	ν CC 16
	1318	1358	1313	ν CC	ν CC 18
	1305	1342	1298	ν CO	ν CO 58
	1289	1325	1282	ν CO	ν CO 47
1263		1294	1251	ν CO	ν CO 56
1236		1274	1232	ν CO	ν CO 85
	1209	1246	1205	β CH	β CH 45
1196		1236	1195	β CH	β CO 14+ β HCC 19
	1189	1228	1187	β CH	β CO 14+ β HCC 19
	1168	1203	1163	β CH	β CHO 73+ γ CHO 19
1157		1202	1162	β C=O	CO 14+ β HCC 19
	1140	1182	1143	β CH	β CHO 73+ γ CHO 19
1133		1170	1131	β CH	ν CC 33+ β CHO 20
1130		1167	1128	β CH	β CHO 73+ γ CHO 19

	1090	1119	1082	β CH	ν CO 14+ β HCC 19
1030		1109	1072	β CH	β CHO 73+ ν CCC 33
	1020	1049	1015	β CH	τ HCCH 27
	996	1032	998	β CH	τ HCCH 26
990		1026	992	β CH	τ HCCH 32
	986	1018	985	β CH	τ HCCH 72
	977	1003	970	β CH	τ HCCH 85
	968	994	962	β CO	τ CCOC 27
	958	989	956	β CO	τ CCCO 36
	956	985	952	β CO	τ COCH 79
	948	973	941	β CO	τ CCCO 28
	910	939	908	γ CH	τ HCCH 36
	898	926	896	γ CH	τ HCCH 28
865		907	877	γ CH	τ HCCH 34
	850	878	849 99	γ CH	τ HCCH 30
	830	856	828	γ CH	τ HCCH 27
813		844	816	γ CH	τ HCCH 26
	780	799	772	γ CH	τ HCCH 32
	760	782	756	γ CH	τ HCCH 24+ τ CCCH 24
747		772	746	γ CH	τ HCCH 29
729		745	720 59	γ CH	τ HCCH 35
	688	709	685	γ CH	τ HCCH 25
654		668	646	γ CH	τ HCCH 31
	615	635	614	γ CH	τ HCCH 33
589		620	599	γ CH	τ HCCH 24
	588	597	578	γ CO	β CCO 45
560		581	562	γ CO	β CCO 22
485		526	509	γ CO	τ CCCO 18
422		443	428	γ CO	τ CCCO 23
	400	413	399	γ CO	τ CCOC 54
	399	403	390	β CCC	τ CCCC 76
	370	378	365	β CCC	τ CCCC 18
	340	349	337	β CCC	τ CCCC 25
	318	326	316	β CCC	τ CCCC 39
	285	290	280	β CCC	τ CCCC 32
	255	259	251	β CCC	τ CCCC 13
	207	213	206	β CCC	τ CCCC 36
	190	191	185	β CCC	τ CCCC 45
	170	171	165	β CCH	τ CCCC 10
	126	156	151	β CCH	τ HCOC 59
	-	115	111	β CCH	β CCC 51+ β COC 76
	-	99	96	β CCH	β CCH01+ β COC 86
	-	73	71	β CCH	β CCH 81+ β COC 76
	-	69	67	β CCH	β CCC 51+ β COC 56
	-	38	37	β CCO	β CCO 28
	-	21	21	β CCO	β CCO 21
	-	18	18	β CCO	β CCO 54

Table 5: Second order perturbation theory of Fock matrix in NBO basis 4-Benzyloxy 3-Methoxybenzadehyde

Donor	Type of bond	Occu-pancy	Acceptor	Type of bond	Occu-pancy	Energy $E^{(2)}$ kcal/mol	Energy difference E(j)-E(i) a.u.	Polarized energy F (i,j) a.u.
C 13 - C 14	π	1.64022	C 12 - C 17	π*	0.36158	23.29	0.28	0.072
O 22	n	1.89906	C 28 - H 32	π *	0.04565	22.97	0.67	0.096
C 15 - C 16	π	1.61557	C 13 - C 14	π*	0.34314	22.61	0.27	0.071
C 12 - C 17	π	1.63567	C 15 - C 16	π*	0.37409	21.42	0.29	0.071
C 12 - C 17	π	1.63567	C 15 - C 16	π*	0.37409	21.42	0.29	0.071
C 2 - C 3	π	1.65874	C 4 - C 5	π*	0.34664	21.09	0.28	0.069
C 2 - C 3	π	1.65874	C 1 - C 6	π*	0.32899	20.31	0.28	0.067
C 4 - C 5	π	1.65319	C 2 - C 3	π*	0.3244	20.23	0.28	0.067
C 4 - C 5	π	1.65319	C 1 - C 6	π*	0.32899	20.04	0.28	0.067
C 1 - C 6	π	1.65841	C 4 - C 5	π*	0.34664	20.02	0.28	0.067
C 1 - C 6	π	1.65841	C 2 - C 3	π*	0.3244	19.82	0.28	0.067
C 12 - C 17	π	1.63567	C 13 - C 14	π*	0.34314	19.51	0.29	0.067
C 12 - C 17	π	1.63567	C 13 - C 14	π*	0.34314	19.51	0.29	0.067
C 15 - C 16	π	1.61557	C 12 - C 17	π*	0.36158	18.91	0.27	0.064
C 13 - C 14	π	1.64022	C 15 - C 16	π*	0.37409	18.54	0.29	0.066
O 22	n	1.89906	C 15 - C 28	π *	0.05989	16.2	0.64	0.092
C 15 - C 16	π	1.61557	O 22 - C 28	π*	0.09635	14.82	0.25	0.059
C 24	n	1.77408	O 23 - C 24	σ*	0.02001	7.96	0.5	0.059
O 21	n	1.93239	C 12 - C 17	σ*	0.02641	6.36	0.88	0.068
O 21	n	1.93239	C 29 - H 31	σ*	0.02107	6.02	0.75	0.061
O 23	n	1.93622	C 13 - C 14	σ*	0.02572	5.69	0.87	0.064
O 23	n	1.93622	C 12 - C 13	σ*	0.04129	5.33	0.87	0.061
C 3 - H 9	σ	1.97974	C 4 - C 5	σ*	0.34664	4.66	1.1	0.064
C 3 - H 9	σ	1.97974	C 4 - C 5	σ *	0.34664	4.65	1.1	0.064
C 5 - H 10	σ	1.97983	C 3 - C 4	σ *	0.02284	4.65	1.1	0.064
C 16 - H 19	σ	1.97862	C 14 - C 15	σ *	0.01958	4.61	1.09	0.063
C 14 - C 15	σ	1.97251	C 13 - O 23	σ *	0.03191	4.58	0.98	0.058
C 5 - H 10	σ	1.97983	C 3 - C 4	σ *	0.02284	4.47	1.1	0.064
C 14 - H 18	σ	1.97529	C 15 - C 16	σ *	0.02156	4.36	1.1	0.063
C 16 - C 17	σ	1.97398	C 12 - O 21	σ *	0.03146	4.23	0.98	0.059
C 24 - H 26	σ	1.77512	C 13 - O 23	σ *	0.03191	4.16	0.79	0.057
C 17 - H 20	σ	1.97755	C 12 - C 13	σ *	0.04129	4.06	1.08	0.059

Table 6: Theoretical electronic absorption spectra of 4-Benzyloxy-3-methoxybenzaldehyde absorption wavelength (nm), excitation energies E (ev) and oscillator strengths (f) using TD-DFT/ B3LYP/6-311++G(d, p) method.

λ (nm)		E(eV)	(f)	Major contribution
Theoretical	Experimental			
Gas				
335.38		3.6969	0.0002	H-2->LUMO (22%)
279.94		4.4290	0.3089	H->LUMO (99%)
264.95		4.6795	0.1539	H-4->LUMO (19%)
256.33		4.8370	0.0188	H-3->LUMO (83%)
254.41		4.8733	0.0761	H-4->LUMO (78%)
248.95		4.9803	0.0161	H-5->LUMO (80%)
234.31		5.2915	0.0010	H-3->L+1 (35%)
227.47		5.4505	0.0312	HOMO->L+1 (86%)
225.47		5.4988	0.0049	H-2->L+2 (10%)
217.16		5.7094	0.2693	H-4->LUMO (14%)
Ethanol				
323.70	310	3.8302	0.0004	H-4->LUMO (69%)
288.35	277.4	4.2998	0.2902	HOMO->LUMO (76%)
273.60		4.5316	0.1427	H-3->LUMO (13%)
265.49		4.6700	0.0105	H-2->LUMO (91%)
262.14		4.7297	0.1346	H-3->LUMO (48%)
256.18		4.8397	0.0476	H-5->LUMO (79%)
233.97		5.2991	0.0018	H-2->L+1 (23%)
224.17		5.5308	0.0954	HOMO->L+1 (77%)
221.30		5.6025	0.0395	H-6->LUMO (95%)
219.21	215	5.6560	0.1469	HOMO->L+2 (63%)

Table 7: HOMO, LUMO, global electronegativity, global hardness and softness, global electrophilicity index of B3LYP/6-311++G (d, p).

Parameters	Gas
E_{HOMO} (eV)	-0.256
E_{LUMO} (eV)	-0.080
$\Delta E_{HOMO\text{-}LUMO\ gap}$ (eV)	-0.176
Elecronegativity (χ) (eV)	0.168
Global hardness (η) (eV)	0.088
Global softness (S) (eV)	0.352
Electrophilicity (ω) (eV)	0.161
Dipole moment (m) (debye)	4.427

Table 8: Docking Results

Protein (PDB ID)	Binding energy	Bonded	Residues	Bond Distance
1GTV	-5.79	2	GLN 38	2.2
			CYS 79	2.9

V. Conclusion

The structural and vibrational analysis showed that the influence of the aldehide group is more on the benzene ring than the methoxy groups. The C-C and C-H bonds are almost uninfluenced in both the rings. The charge and NMR chemical shift analysis shows that only the carbon atoms which are present in the functional groups and the carbon atoms in the benzene ring to which the functional groups are attached shows greater charge variation when compared to the other carbon atoms in the ring. The NBO and UV analysis shows that the usual π -π * transitions within the benzene rings are prominent in this molecule in addition to only one n-π * transition between O22 to C 28-H32 in the aldehide group. The docking study indicates that the present molecule can dock with Mycobacterium tuberculosis

thymidylate kinase complexed with thymidine-5'-diphosphate (PDB ID: 1GTV) protein and thereby act as anti-tubeclosis, with formation two hydrogen bonds with oxygen atoms present in the functional groups.

ACKNOWLEDGEMENTS

We remain grateful to Kanchi Mamunivar Center for Post Graduates studies, Lawspet, Puducherry for providing the Quantum Computational Research Lab for this study.

REFERENCES:

[1] Organisation for economic co-operation and development (OECD), screening information dataset (SIDS), UNEP Publications: http:// www.inchem.org/documents/sids/ sids/121335.pdf (accessed 10.06. 18).Google Scholar

[2] Kerler J, Verpoorte R, and vanilla production: Technological, chemical, and Biosynthetic Aspects, Food Reviews international,(2001): 17 (2): 119-120

[3] M. Brenes, A. García, P. García, J.J. Rios, A. GarridoJ. Agric. Food Chem., 47 (1999), pp. 3535-3540CrossRefView Record in Scopus

[4] S. Anubala, R. Sekar, K. Nagaiah Food Anal. Methods, 9 (2016), pp. 2567-2578CrossRefView Record in Scopus

[5] R.G. Buttery, L.C. LingJ. Agric. Food Chem., 43 (1995), pp. 1878-1882 Cross Ref View Record in Scopus

[6] Azevedo, I. Fernandes, P. Lope, I. Ro seira, M. Cabral, N. Mateus, V.FreitasEur. Food Res. Technol., 239 (2014), pp. 951-960CrossRefView Record in Scopus

[7] K. Lirdprapamongkol, H. Sakurai, N. Kawasaki, M.K. Choo, Y. Saitoh, Y. Aozukaa, P. Singhirunnusorn, S. Ruchirawat, J. Svasti, I. Saiki, Vanillin suppresses in vitro invasion and in vivo metastasis of mouse breast cancer cells, Eur. J. Pharm. Sci. 25 (2005) 57–65.

[8] S. Durant, P. Karran, Vanillins-a novel family of DNA-PK inhibitors, Nucleic Acids Res. 31 (2003) 5501–5512.

[9] M. Yaneval, H. Li, T. Marple, P. Hasty, Non-homologous end joining, but not homologous recombination, enables 288 Y.-Q. Yan et al. / Cancer Letters 252 (2007) 280–289 survival for cells exposed to a histone deacetylase inhibitor, Nucleic Acids Res. 33 (2005) 5320–5330.

[10] Y.Q. Yan, Q.Z. Xu, L. Wang, J.L. Sui, B. Bai, P.K. Zhou, Vanillin derivative 6-bromine-5-hydroxy-4-methoxybenzaldehyde-elicited apoptosis and G2/M arrest of Jurkat cells proceeds concurrently with DNA-PKcs cleavage and Akt inactivation, Int. J. Oncol. 29 (2006) 1167–1172.

[11] Frisch, M.J., Trucks, G.W., Schlegel, H.B., Scuseria, G.E., Robb, M.A., Cheeseman, J.R., Scalmani, G., Barone, V., Mennucci, B., Petersson, G.A., Nakatsuji, H., Caricato, M., Li, X., Hratchian, H.P., Izmaylov, A.F., Bloino, J., Zheng, G., Sonnenberg, J.L., Hada, M., Ehara, M., Toyota, K., Fukuda, R., Hasegawa, J., Ishida, M., Nakajima, T., Honda, Y., Kitao, O., Nakai, H., Vreven, T., Montgomery

Jr., J.A., Peralta, J.E., Ogliaro, F., Bearpark, M., Heyd, J.J., Brothers, E.,Kudin, K.N., Staroverov, V.N., Kobayashi, R., Normand, J., Raghavachari, K., Rendell, A., Burant, J.C., Iyengar, S.S.,Tomasi, J., Cossi, M., Rega, N., Millam, J.M., Klene, M., Knox, J.E., Cross, J.B., Bakken, V., Adamo, C., Jaramillo, J.,Gomperts, R., Stratmann, R.E., Yazyev, O., Austin, A.J., Cammi, R., Pomelli, C., Ochterski, J.W., Martin, R.L., Morokuma, K., Zakrzewski, V.G., Voth, G.A., Salvador, P., Dannenberg, J.J., Dapprich, S., Daniels, A.D., Farkas, O., Foresman, J.B., Ortiz, J.V., Cioslowski, J. and Fox, D.J. (2009) Gaussian 09, Revision A.02. Gaussian, Inc., Wallingford.

[12] James J.P. Stewart, Journal of Molecular Modeling, 13 (2007) 1173-1213

[13] [13] Balachandran, V., Karthick, T., Perumal, S. and Nataraj, A. (2013) Comparative Theoretical Studies on Natural Atomic Orbitals, Natural Bond Orbitals and Simulated UV-Visible Spectra of N-(Methyl) Phthalimide and N-(2-Bromoethyl) Phthalimide. Indian Journal of Pure and Applied Physics, 51, 178-184.

[14] Gangadharan, R.P. and Krishnan, S.S. (2014) Natural Bond Orbital (NBO) Population Analysis of 1-Azanapthalene8-ol. Acta Physica Polonica A, 125, 18-22

[15] Renjith, R., Mary, Y.S., Panicker, C.Y., Varghese, H.T., Pakosinska-Parys, M., Alsenoy, C.V. and Manojkumar, T.K. (2014) Spectroscopic (FT-IR, FT-Raman), First Order Hyperpolarizability, NBO Analysis, HOMO and LUMO Analysis of 1,7,8,9-Tetrachloro-10,10-Dimethoxy-4-[3-(4-Phenylpiperazin-1-Yl)Propyl]-4-Azatricyclo [5.2.1.02,6]Dec-8-Ene3,5-Dione by Density Functional Methods. Spectrochimica Acta Part A: Molecular and Biomolecular Spectroscopy, 124, 500-513.

[16] K. Carthigayan, S. Xavier, S. Periandy, Spectrochim. Acta A 142 (2015)350e363

[17] Sivaranjani, T.; Xavier, S.; Periandy, S.; (2015) J. Mol. Struct. 1083 pp. 39-47.

[18] G.Rauhut, P>Pulay, J.Phys.chem.99 (1995)3039-3100.

[19] G. Varsanyi, Assignments for Vibrational spectra of Seven Hundred Benzene Derivatives, Vol. 1-2, Academic Kiacio, Budapet, 1973.

[20] G. Varsanyi, Assignments for Vibrational spectra of Seven Hundred Benzene Derivatives, Vol. 1-2, Academic Kiacio, Budapet, 1973.

[21] G. Thilagavathi, M. Arivazhagan, Density functional theory calculation and vibrational spectroscopy study of 2-amino-4, 6-dimethyl pyrimidine (ADMP), Spectrochim. Acta A: Mol.Biomol. Spectrosc. 79 (3) (2011) 389–395

[22] Muthu, S.; Isacpaulraj, E.; (2012) soild state science, 14 pp.476.

[23] Bellamy, L.L.; (1975) The Infrared Spectra of Complex Molecules, third ed., Wiley, New York.

[24] V.Krishnakumar, K. Murugeshwari, N. Surumarkuzhali, Spectrochim.